



Cite this: *Environ. Sci.: Processes Impacts*, 2025, 27, 2740

## Drivers and riverine fluxes of rare earth elements to coastal ecosystems across temperate, boreal, and subarctic ecoregions in Eastern Canada†

Marie-Christine Lafrenière, <sup>a</sup> Md Samrat Alam, <sup>ab</sup> Jean-François Lapierre, <sup>a</sup> Dominic E. Ponton, <sup>a</sup> Maxime Wauthy, <sup>a</sup> Caroline Fink-Mercier, <sup>c</sup> Holly Marginson, <sup>a</sup> Paul del Giorgio<sup>c</sup> and Marc Amyot <sup>\*a</sup>

Although rivers are recognized as major transporters of REEs to coastal environments, estimates of REE fluxes are still scarce, and the underlying drivers remain poorly understood—particularly in temperate, boreal, and subarctic river systems. This limits our understanding of the global REE cycle and limits our ability to identify or predict increases in exports driven by climate change or anthropogenic activities, which could pose a threat to biodiversity. This study aims to calculate and compare lotic REE fluxes and yields in 40 rivers draining watersheds with different geologies and climates within the Province of Quebec ( $\sim 1.5 \text{ M km}^2$ ), Canada. Furthermore, we observed their differences in REE composition as well as the main factors driving their concentrations. We estimated the annual export of total REEs flowing into the Hudson Bay (1078 t per year) and the Atlantic Ocean (2941 t per year), which could increase significantly with climate change effects on the northern ecosystems. From these watersheds, rivers draining the Canadian Shield geology, characterized by lower water temperature and pH, but higher concentrations of dissolved organic carbon (DOC) and iron (Fe), exhibited higher concentrations of REEs compared to the broader study area, especially filtered light REEs (LREEs). In southern Quebec, rivers with intensive agricultural erosion were identified as REE export hotspots relative to their watershed area, while rivers draining densely populated regions exported anthropogenic gadolinium (Gd) (0.2–134 kg per year), contributing significantly to their total filtered Gd flux (18–98%). These findings provide essential baseline data to predict regional impacts of climate changes and anthropogenic activities on REE mobilization across evolving landscapes and clarify the role of temperate, boreal and subarctic rivers in the global REE cycle.

Received 22nd May 2025  
Accepted 4th July 2025

DOI: 10.1039/d5em00391a  
[rsc.li/espi](http://rsc.li/espi)

### Environmental significance

Rare earth elements (REEs) are essential to modern technologies and the global energy transition. Their growing extraction, combined with climate-driven changes in precipitation and erosion, is disrupting their natural biogeochemical cycle. Understanding how REEs are transferred across the land-to-aquatic continuum, from terrestrial ecosystems to freshwater and ultimately coastal and marine ecosystems, is essential to assessing their long-term environmental fate and impacts. This study quantifies REE fluxes and yields across temperate, boreal, and subarctic watersheds covering 1.5 million  $\text{km}^2$ , providing critical insights into their biogeochemical cycling and helping to close key knowledge gaps in the global REE cycle. Findings reveal how land use, geology, and climate factors influence both REE export and solubility, affecting their bioavailability and potential toxicity in aquatic ecosystems. This work provides new insight into how changing environmental pressures may shape the fate of REEs in northern river systems.

### Introduction

Rivers are crucial for coastal and marine productivity, supplying nutrients, terrestrial materials, and trace metals, including rare earth elements (REEs), a group of 17 metals of emerging interest. The growing demand for high technology has accelerated global REE exploitation, disrupting their natural cycle and enriching some REEs in aquatic environments,<sup>1–3</sup> where they may pose ecotoxicological risks.<sup>4</sup> For instance, in addition to potential acute toxicity, REEs have been shown to cause

<sup>a</sup>Groupe Interuniversitaire en Limnologie et en Environnement Aquatique (GRIL), Département des Sciences Biologiques, Université de Montréal, Montréal, Quebec, Canada. E-mail: [m.amyot@umontreal.ca](mailto:m.amyot@umontreal.ca)

<sup>b</sup>Geological Survey of Canada, Natural Resources Canada, Quebec, Canada

<sup>c</sup>Groupe Interuniversitaire en Limnologie et en Environnement Aquatique (GRIL), Département des Sciences Biologiques, Université du Québec à Montréal, Montréal, Quebec, Canada

† Electronic supplementary information (ESI) available. See DOI: <https://doi.org/10.1039/d5em00391a>



sublethal effects, such as developmental abnormalities and cytotoxicity, in a variety of aquatic organisms.<sup>5–7</sup> Although recent studies highlight rivers and continental margin sediments as key sources and processors of REEs to coastal environments,<sup>8–12</sup> the dynamics of REE fluxes remain poorly understood, especially in temperate, boreal and subarctic rivers. In these northern rivers, climate change effects such as rapid warming, ice cap melting, permafrost thaw and shifts in precipitation, and their impact on the transport and quality of aquatic dissolved organic matter, might also enhance the mobilization of organic matter bound REEs from terrestrial to marine ecosystems in the coming decades.<sup>13,14</sup> Understanding REE fluxes is crucial for predicting how large-scale changes and increasing anthropogenic influence will affect their mobilization and relative composition, while also improving our knowledge of their global cycling, which currently has missing sources and may be biased by the underrepresentation of northern ecosystems in existing estimates.<sup>12,15,16</sup>

Most studies on REE fluxes focus on dissolved neodymium (Nd), often using its  $^{143}\text{Nd}/^{144}\text{Nd}$  isotope ratio to trace water mass mixing. These studies reveal the significance of continental filtered fluxes in the global marine REE budget.<sup>8–10</sup> For example, the Amazon River contributes 14% to 30% of the dissolved neodymium to the Atlantic Ocean (607–1227 t per year), with similar estimates for the Congo (547  $\pm$  183 t per year) and Orinoco Rivers (336 t per year).<sup>8,17,18</sup> Since most REEs in rivers are bound to colloids and particles, measuring particulate or total REE fluxes is essential, as such data are currently lacking in the literature.<sup>19–21</sup> In addition, our understanding of the fluxes and large-scale dynamics of other REEs remains incomplete, as neodymium alone does not accurately represent the behavior of the entire series. Although REEs share similar trivalent behavior, environmental fractionation between LREEs and HREEs along with redox-sensitive anomalies, can lead to distinct environmental patterns and budgets, particularly under varying conditions, geological settings and anthropogenic pressures.<sup>22–24</sup>

Monitoring REE fluxes to coastal environments is increasingly important as anthropogenic activities introduce more REEs into river systems. This is particularly relevant for gadolinium (Gd) from MRI contrast agents, whose fluxes are constantly increasing in multiple rivers draining densely populated areas, regardless of discharge rates,<sup>25–27</sup> complicating the use of predictive models. For instance, annual anthropogenic Gd fluxes from the Rhine River to the North Sea are estimated at 730 kg, yet their environmental impacts remain unclear.<sup>3</sup> In addition to Gd, significant fluxes of lanthanum (La) (5700 kg) and samarium (Sm) (584 kg) arise from catalyst production in petroleum refining industries (Kulaksiz and Bau, 2013). Other sources, such as human-driven erosion<sup>28</sup> and hydrological alterations from damming or diversion, further complicate the understanding of REE dynamics in riverine systems and limit our ability to distinguish anthropogenic REE fluxes from natural REE fluxes. Given the anticipated rise in urban development and associated ecosystem modifications, there is a pressing need to quantify the specific pathways and

magnitudes of anthropogenic REE fluxes to coastal ecosystems to better constrain their role in the global biogeochemical cycle.

River outlets provide crucial insight into combined sources, processes and sinks of trace elements in watersheds. Rare earth elements are primarily delivered to temperate or boreal rivers during high-flow events, often transported with organic ligands or Fe- and Mn-rich colloids.<sup>20,29–31</sup> Their fate is then influenced by river water chemistry, especially pH which affects their solubility and adsorption to oxyhydroxides. Lighter REEs are bound more readily to these oxyhydroxides, increasing their sedimentation, while heavier REEs form stronger complexes either with carbonates or dissolved organic matter, remaining in solution.<sup>29,30</sup> Additionally, these oxyhydroxide precipitates may release REEs back into the water column through dissolution or sediment remobilization and even contribute to a significant sedimentary flux towards coastal environments.<sup>10,32</sup> In alkaline rivers, REEs complexed with organic ligands and carbonates are more stabilized, reducing removal by saline coagulation in downstream estuarine environments.<sup>32</sup> Watershed geology also affects REE fluxes by acting as a source or influencing water chemistry. For example, variations in discharge in the Orinoco River, which drains silicate and carbonate rocks, alter pH, organic matter and oxyhydroxide influx, thereby controlling REE concentrations.<sup>17</sup> Furthermore, river water chemistry directly modulates the flux of REEs delivered to coastal ecosystems by affecting REE solubility, sedimentation processes, and estuarine removal. As global warming affects watershed hydrology and river metabolism (e.g., pH and DOC), it is essential to understand how these factors change the magnitude and the relative composition of REE fluxes.

Canada's vast freshwater resources, including those trapped in glaciers and permafrost, and its significant REE reserves (>15.1 million tons of REE oxides)<sup>33</sup> highlight the importance of estimating REE fluxes across the Canadian landscape towards estuarine ecosystems, where REEs may accumulate.<sup>34</sup> The high hydrological connectivity of these systems may promote long-range transport of REEs between distant ecosystems, particularly in the context of climate change and increasing local exploitation,<sup>13,14</sup> potentially positioning Canada as a major REE export hotspot. Quantifying REE export from freshwater systems is therefore essential to evaluate potential downstream impacts and support sustainable resource management. In this study, we estimate and compare REE fluxes and yields in 40 rivers across different geological and climatic regions in Quebec, Canada, and identify the main factors, such as pH and temperature, as well as dissolved organic carbon (DOC) and Fe, Mn, and Al concentrations, influencing their concentrations and relative composition. In addition, we calculated fluxes of anthropogenic Gd and investigated the effects of dams on REE export, which are present in numerous Quebec river systems.

## Methods

### Study area

During the late spring and summer periods of 2017 to 2020, samples were collected from the mouths of 40 rivers across



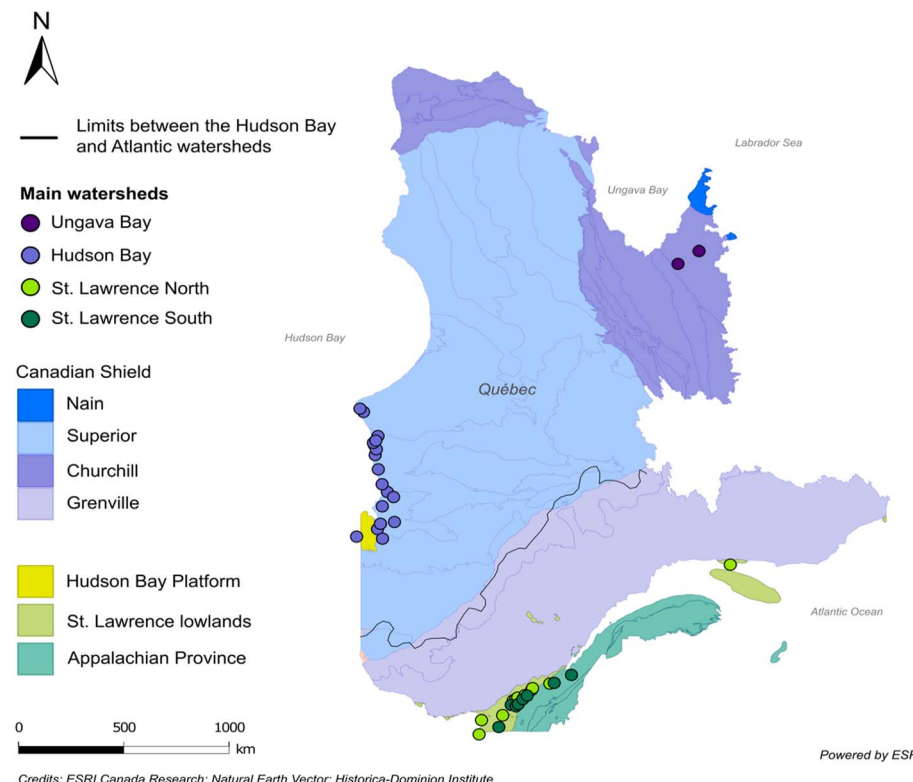


**Fig. 1** Map of the study area, with site locations of rivers draining different watersheds from the Province of Québec, namely the Ungava Bay ( $n = 2$ ), the Hudson Bay ( $n = 18$ ), the north of the St. Lawrence River ( $n = 8$ ) and the south of the St. Lawrence River ( $n = 12$ ), colored according to geographical provinces. Sampling locations are represented by the dots which are colored according to the main watersheds they drain. The solid black line delimits the Hudson Bay and the Atlantic watershed. Credits: ESRI Canada, Natural Earth Vector, ESRI Canada, Historica-Dominion Institute. The map was created using ArcGIS by ESRI.

various ecoregions in the Province of Quebec, Canada, namely the southern Mixedwood Plains,<sup>10</sup> the Boreal Shield,<sup>10</sup> the Taiga Shield<sup>18</sup> and the low arctic tundra<sup>4</sup> (Fig. 1 and Table 1). The hydrological network spans two primary drainage basins: one covering 919 393 km<sup>2</sup> flows toward Hudson Bay and the Arctic Ocean, while another 576 591 km<sup>2</sup> drains into the Northeast Atlantic Ocean. From the Hudson Bay watershed, most of the sampled rivers first empty into the James Bay while the George and Koroc Rivers flow further north into the Ungava Bay. From the Atlantic Ocean watershed, all rivers empty into the St. Lawrence River, except for La Romaine that empties into the St. Lawrence Estuary. To capture variation in these watersheds, we have grouped rivers draining either into the Hudson Bay, Ungava Bay or St. Lawrence River (North or South shore) watersheds. Most of the sampled rivers drain the Canadian Shield, a geologic region composed of Precambrian rocks enriched in REEs, except for the rivers south of the St. Lawrence River, which flow through the productive agricultural lands of the St. Lawrence Lowlands platform and the sedimentary basin of the Appalachian region (SIGÉOM).<sup>35,36</sup> Although the Yamachiche River and Bayonne River are north of the St. Lawrence River, they exclusively drain the St. Lawrence lowlands; therefore they were integrated in the groups of rivers south of the St. Lawrence River. In this paper, we categorized the rivers as “dammed” if their impounding capacity was greater than 1 000 000 m<sup>3</sup> ( $n = 14$ ). We followed methods from Wauthy and

Amyot<sup>37</sup> and excluded the Au Castor, Eastmain, Pontax, Rupert and St. Lawrence rivers from this classification, since the sampled water does not originate from a large reservoir.

## Data collection

This study gathered data from published work, that is, REE concentrations and water chemistry variables from the St. Lawrence River and its tributaries<sup>21</sup> and from the George River and Koroc River.<sup>38</sup> We also included water chemistry variables and unpublished data from 18 rivers draining the Eastern James Bay<sup>39</sup> and from the Romaine River.<sup>40</sup>

Historical discharge data for most of the St. Lawrence tributaries were obtained from an online database from Gouvernement du Québec,<sup>41</sup> the Atlas hydroclimatique, and originate from hydrometric stations and hydrological modelling using the optimal interpolation method.<sup>42</sup> We chose the most recent ten-year period available for mean annual discharge. For discharge upstream of the St. Lawrence River, we used Lake Ontario outflow changes from International Lake Ontario-St. Lawrence River Board monitoring.<sup>43</sup> For downstream, we used discharge at Quebec City, which was calculated by Fisheries and Oceans Canada.<sup>44,45</sup> Ottawa River discharge was taken at the Carillon dam station.<sup>46</sup> For rivers draining the James Bay, mean annual discharges were obtained from Fink-Mercier and Lapierre<sup>39</sup> derived from both hydrometric stations in gauged rivers



Table 1 Physical and chemical data<sup>a</sup> of sampled rivers from the Province of Quebec

| River   | n <sup>a</sup> | Discharge (m <sup>3</sup> s <sup>-1</sup> ) | Watershed area (km <sup>2</sup> ) | Temperature (°C) | pH   | Specific conductivity (μS cm <sup>-1</sup> ) | DOC (mg L <sup>-1</sup> ) | Filtered REEs <sup>b</sup> (μg L <sup>-1</sup> ) | Total REEs <sup>b</sup> (μg L <sup>-1</sup> ) |
|---|----------------|---|-----------------------------------|------------------|------|--|---------------------------|--|---|
| <b>Atlantic watershed – north</b>             |                |   |                                   |                  |      |  |                           |  |   |
| Assomption                                    | 2              | 19  | 4333                              | 22.8             | 7.8  | 162.5  | 5.1                       | 0.48   | 2.59  |
| Batiscan                                      | 2              | 99  | 4690                              | 17.4             | 7.2  | 150.2  | 4.6                       | 1.10   | 1.92  |
| Bayonne                                       | 1              | 4   | 352                               | 19.9             | 6.8  | 233.2  | 4.2                       | 0.29   | 2.81  |
| Du Loup                                       | 2              | 27  | 1610                              | 17.6             | 7.3  | 83.3   | 4.2                       | 0.95   | 4.83  |
| La Romaine                                    | 2              | 280   | 14 470                            | 13.8             | 6.0  | 14.3   | 6.6                       | 1.04   | —   |
| Maskinongé                                    | 2              | 19  | 1105                              | 17.1             | 7.6  | 58.3   | 6.0                       | 0.77   | 2.48  |
| Ottawa  | 2              | 2148  | 146 300                           | 21.1             | 7.9  | 72.0   | 7.0                       | 0.89   | 2.03  |
| Sainte-Anne                                   | 1              | 51  | 2706                              | 16.4             | 6.4  | 63.3   | 4.2                       | 0.98   | 1.79  |
| Saint-Maurice                                 | 4              | 670   | 43 300                            | 24.6             | 6.9  | 64.8   | 6.9                       | 1.30   | 2.01  |
| St. Lawrence                                  | 4              | 12 563                                      | 1 344 200                         | 25.1             | 8.0  | 269.1  | 3.2                       | 0.07   | 1.87  |
| Yamachiche                                    | 2              | 5   | 266                               | 15.3             | 7.4  | 1571.5                                       | 8.7                       | 1.10   | 4.69  |
| <b>Atlantic watershed – north</b>             |                |   |                                   |                  |      |  |                           |  |   |
| Boyer   | 1              | 4   | 217                               | 15.6             | 7.9  | 304.3  | 4.4                       | 0.29   | 27.42   |
| Becancour                                     | 2              | 48  | 2620                              | 18.9             | 8.2  | 204.5  | 6.0                       | 0.30   | 2.63  |
| Châteauguay                                   | 1              | 38  | 2501                              | 20.7             | 9.4  | 286.6  | 4.3                       | 0.05   | 0.40  |
| Chaudière                                     | 1              | 123   | 6682                              | 14.3             | 6.7  | 203.5  | 5.4                       | 0.10   | 0.29  |
| Nicolet                                       | 2              | 33  | 3380                              | 19.7             | 8.0  | 296.0  | 5.6                       | 0.49   | 13.09   |
| Richelieu                                     | 2              | 392   | 23 720                            | 19.3             | 8.3  | 169.7  | 3.5                       | 0.10   | 1.95  |
| Saint-Regis                                   | 2              | 37  | 93                                | 16.4             | 8.3  | 1534.0                                       | 4.44                      | 0.16   | 1.57  |
| Saint-François                                | 1              | 163   | 10 230                            | 19.6             | 8.1  | 209.2  | 7.8                       | 0.21   | 0.87  |
| Yamaska                                       | 2              | 65  | 4784                              | 18.2             | 8.5  | 352.6  | 6.7                       | 0.19   | 5.88  |
| <b>Hudson Bay watershed – James Bay area</b>  |                |   |                                   |                  |      |  |                           |  |   |
| Aquatic                                       | 2              | 2   | 188                               | 12.0             | 6.4  | 39.7   | 20.3                      | 2.89   | 3.59  |
| Beaver  | 2              | 25  | 2941                              | 8.7              | 6.8  | 26.3   | 9.5                       | 0.80   | 1.22  |
| Broadback                                     | 2              | 329   | 20 808                            | 17.8             | 6.6  | 25.5   | 10.0                      | 1.49   | 3.02  |
| Caillet                                       | 2              | 6.3   | 470                               | 13.0             | 6.7  | 42.8   | 17.4                      | 2.24   | 3.61  |
| ChinuSAW                                      | 2              | 0.5   | 44                                | 11.3             | 6.5  | 112.5  | 21.8                      | 1.41   | 3.32  |
| Conn  | 2              | 10.5  | 691                               | 15.1             | 6.8  | 40.2   | 15.4                      | 2.25   | 3.44  |
| Eastmain                                      | 2              | 30.3  | 3973                              | 12.5             | 6.07 | 22.5   | 14.1                      | 3.57   | 6.28  |
| Guillaume                                     | 2              | 13.3  | 1183                              | 12.8             | 6.6  | 36.8   | 18.9                      | 3.19   | 4.55  |
| Harricana                                     | 2              | 325   | 29 418                            | 17.0             | 7.7  | 132.5  | 13.9                      | 1.49   | 4.1   |
| Jolicoeur                                     | 2              | 14  | 1777                              | 11.9             | 6.6  | 113.4  | 16.5                      | 1.60   | 2.79  |
| La Grande                                     | 2              | 3133  | 209 453                           | 7.4              | 6.3  | 11.2   | 4.3                       | 0.55   | 0.85  |
| Maquata                                       | 2              | 14  | 1036                              | 16.5             | 7.5  | 25.0   | 12.5                      | 1.02   | 1.51  |
| Nottaway                                      | 2              | 1082  | 62 159                            | 18.5             | 6.9  | 25.7   | 12.0                      | 1.82   | 3.25  |
| Old Factory                                   | 2              | 32  | 2723                              | 14.9             | 6.5  | 28.6   | 12.0                      | 1.52   | 2.12  |
| Pontax  | 2              | 100   | 7894                              | 15.7             | 6.7  | 35.8   | 13.5                      | 1.85   | 4.85  |
| Rupert  | 2              | 239   | 11 596                            | 17.7             | 6.7  | 16.2   | 5.7                       | 0.66   | 1.68  |
| Salmon  | 2              | 0.8   | 69                                | 7.9              | 7.3  | 896.0  | 6.6                       | 0.15   | 0.32  |
| Seal  | 2              | 35  | 1575                              | 13.3             | 7.0  | 60.3   | 4.2                       | 0.50   | 0.87  |
| <b>Hudson Bay watershed – Ungava Bay area</b> |                |   |                                   |                  |      |  |                           |  |   |
| George River                                  | 5              | 829   | 41 699                            | 11.0             | 6.9  | 9.88   | 2.3                       | 0.63   | 0.78  |
| Koroc River                                   | 3              | 199   | 10 000                            | 15.8             | 6.6  | —  | 1.1                       | 0.38   | 0.89  |

<sup>a</sup> Data represent mean discharge and mean concentrations based on triplicate samples collected across multiple years (n = number of campaigns/years of sampling). <sup>b</sup> For individual concentrations of REEs see the complete dataset on Borealis, the Canadian Dataverse Repository, at <https://doi.org/10.5683/SP3/E0A6SF>.

and from a linear model using the relationship between mean annual discharge (Q) model based on hydrometric stations and using watershed area (km<sup>2</sup>) ( $R^2 = 0.99$ ; eqn (1), n = 12) (eqn (1)).<sup>47</sup> With this model, we estimated the discharge of the George River, Koroc River, and Assomption River.

$$Q = 0.0084 \times \text{watershed area}^{1.08} \quad (1)$$

### Water sampling and analysis

Physical and chemical parameters, such as temperature, pH, specific conductivity, and dissolved oxygen were measured with a multi-probe YellowSpring Instrument (YSI; Springfield, Ohio). Surface water was sampled near the mouth of the rivers to measure concentrations of major cations and trace metals, including REEs and dissolved organic carbon (DOC) (Table 1).



For trace metal sampling, all equipment was pre-washed with hydrochloric acid 10% (v/v) overnight, and ultratrace techniques were used in the field. For Hudson Bay, water samples were collected either from a boat or by hand, sometimes from a hovering helicopter. While most samples were filtered on-site through a 0.45  $\mu\text{m}$  in-line polycarbonate filter, hand-grabbed samples were filtered with a polycarbonate membrane (0.45  $\mu\text{m}$ , Whatman) mounted on an acid-washed Teflon filtration tower.<sup>39</sup> For the St. Lawrence River, surface water was sampled from a boat with an acid-washed Teflon Kemmerer and immediately filtered with plastic syringes and certified metal-free polyethersulfone filters (0.45  $\mu\text{m}$ , Whatman). The same filtration method was used for the Ungava Bay sampling, but samples were collected either from a boat or a hovering helicopter. Filtered samples comprise both true dissolved (<3 kDa) and colloidal fractions, necessitating caution when interpreting the results. Although the filters are certified as metal-free, they may still adsorb dissolved metals, potentially introducing bias to the concentrations.<sup>48</sup> Field blanks were collected to verify for potential contamination, with approximately 90% of results falling below the limit of detection (LoD) for REEs, calculated as three times the standard deviation of the average of the lowest standards (Table S1†). Samples were preserved at 4 °C with a final concentration of 2% ultra-trace nitric acid (HNO<sub>3</sub>) (EMD, Omnitrace Ultra). In the laboratory, unfiltered samples were digested on a hot plate (2 h, 95 °C) with a final concentration of 3% HNO<sub>3</sub> and 0.5% HCl (EMD, Omnitrace Ultra). Major cations and metals, including all rare earth elements (REEs), iron (Fe), aluminum (Al), and manganese (Mn), were analyzed with triple quadrupole inductively coupled plasma mass spectrometry (8900 ICP-MS/MS, Agilent Technologies). To minimize spectral interference, most REEs were analyzed in oxygen reaction mode (MS/MS) following the approach described in the Agilent Technologies report,<sup>49</sup> while NH<sub>3</sub> mode was used for europium (Eu) to reduce isobaric or polyatomic interference (e.g., with Ba). Helium collision mode was used for other metals. Calibration was verified using river water certified reference material SLRS-6 for trace metals<sup>50</sup> and percentage recoveries (98–116%) were checked for all campaigns for the REE series according to concentrations reported by Yeghicheyan and Aubert.<sup>51</sup> For statistical analysis, values below the LoD were replaced with half the LoD, particularly for summing all REEs<sup>52</sup> (Tables S1–S3†).

For DOC measurements, water samples from Hudson Bay were filtered through 0.45  $\mu\text{m}$  polyethersulfone syringe filters and stored in borosilicate bottles. In the St. Lawrence River system, subsampled water was filtered using glass fiber filters (GF/F) (0.7  $\mu\text{m}$ , Whatman) and stored in pre-combusted (550 °C, 4 h) glass-amber bottles at 4 °C until analysis. Dissolved organic carbon (DOC) measurements were performed with an Aurora 1030 TOC Analyzer (OI Analytical, Texas) or a TIC-TOC analyzer using wet persulfate oxidation (O.I. Corporation, College Station, Texas, USA).

### Estimations of fluxes and yields

To estimate riverine fluxes, the annual mean discharge of rivers was multiplied by REE concentrations. Mean concentrations

were calculated using data from two hydrologically distinct sampling years (2017–2018) in the Atlantic watershed and from 2 to 5 years of filtered concentration data for rivers in the Hudson Bay watershed. Similar to methods described by Wauthy and Amyot,<sup>37</sup> we estimated total REE fluxes from Quebec territory to marine systems. To do that, we first estimated the average specific discharge (discharge-to-catchment area ratio; m per year) of all sampled rivers. We then multiplied this value by the area of the two main watersheds, namely the Hudson Bay watershed (919 393 km<sup>2</sup>), including rivers from the Ungava Bay, and the Atlantic watershed (576 591 km<sup>2</sup>), including rivers from the north and south shores of the St. Lawrence River, to estimate their respective total annual discharge (m<sup>3</sup> per year). This value was then multiplied by the mean metal concentrations from all rivers in each area to estimate their respective annual metal export (metric tons per year). To allow comparisons between rivers independent of discharge, we calculated the yields of REEs as the flux per unit drainage area (kg km<sup>-2</sup> year<sup>-1</sup>). Flux errors represent standard deviations, and error propagation was calculated when errors for both discharge and concentrations were available. If only one error was available, it was multiplied by the multiplicator.

### Standardization of REEs

Standardizing REEs helps identify geochemical processes affecting concentrations across environmental compartments and enables the detection of anthropogenic inputs through anomaly calculations. Concentrations are divided by REE relative abundance in the Earth's crust. Here, we chose the Post-Archean Australian Shale (PAAS).<sup>53,54</sup> Anomalies of Gd (Gd/Gd\*) were quantified using these equations:<sup>55</sup>

$$\text{Gd/Gd}^* = \text{Gd}_{\text{SN}} / (0.5 \text{ Sm}_{\text{SN}} + 0.5 \text{ Dy}_{\text{SN}}) \quad (2)$$

$$(\text{Gd/Gd}^*)_{\text{Eq}(2)} = [\text{Gd}]_{\text{measured}} / [\text{Gd}]_{\text{geogenic}} \quad (3)$$

REE<sub>SN</sub> refers to shale-normalized concentrations while Gd\* refers to its geogenic background. Anthropogenic concentrations and fluxes of Gd were calculated based on eqn (2) when the Gd/Gd\* ratio exceeded 1.4, as natural anomalies are known to occur up to this threshold.<sup>56</sup> To assess enrichment or depletion of light *versus* heavy REEs, we graphically represented the ratios of subgroups representing light ([La + Pr + Nd]<sub>SN</sub>), middle (MREEs; [Sm + Gd + Tb]<sub>SN</sub>) or heavy REEs ([Er + Yb + Lu]<sub>SN</sub>). In the case of rivers that had a pronounced Gd anomaly ( $n = 4$ ), we instead used dysprosium in the calculations of the MREE<sub>SN</sub> subgroup.

### Statistical analyses

Statistical analyses were performed using R version 4.2.2,<sup>57</sup> using functions from the tidyverse,<sup>58,59</sup> ggbreak,<sup>60</sup> FactoMineR,<sup>61</sup> car<sup>62</sup> and oslrf<sup>63</sup> packages. The difference in concentrations between groups (e.g., per watershed or dammed *vs.* undammed) was tested with a non-parametric paired sample Wilcoxon test using the pairwise.wilcox.test() function. To characterize the main drivers of REE concentrations in rivers from each



watershed we performed a principal component analysis (PCA) using `imputePCA()` and `PCA()` functions in type 2 framing with centered-scaled water chemistry variables (pH, temperature, [DOC], [REEs], [Fe] and [Mn]), REE yields and indicators of REE standardized patterns (ratio La:Yb and the Ce anomaly). To further examine the drivers controlling REE concentrations we employed linear regression models using the `lm()` function. Data were log-transformed to meet normality and homoscedasticity assumptions. Multiple linear models were employed with function `ols_step_both_p()` and the correlations between predictors were verified with `cor()` with water quality variables (pH, temperature, conductivity,  $[O_2]$ , [DOC], [TN],  $[SO_4^{2-}]$ ,  $[Cl^-]$ , [Fe] and [Mn]) to test  $[REEs < 0.45 \mu\text{m}]$  and the proportion of them being dissolved.

## Results

### Spatial trend in REE concentrations

We observed increasing filtered REE concentrations ( $[REEs]$ ) going northward of the Province of Quebec, excluding Ungava Bay rivers (Fig. 2). Rivers draining the Hudson Bay and north of the St. Lawrence River watersheds had higher filtered  $[REEs]$  (range =  $0.14\text{--}3.56 \mu\text{g L}^{-1}$ ; mean =  $1.43 \mu\text{g L}^{-1}$ ) compared to rivers draining south of the St. Lawrence River (range =  $0.05\text{--}0.50 \mu\text{g L}^{-1}$ ; mean =  $0.29 \mu\text{g L}^{-1}$ ) ( $p < 0.05$ ) (Fig. 1 and 2 and Table S1†). The small sample size of the Ungava Bay system (range =  $0.38\text{--}0.63 \mu\text{g L}^{-1}$ ;  $n = 2$ ) may reduce the test's statistical power, contributing to the lack of significant differences with other groups. The proportion of filtered REEs followed a similar latitudinal gradient, with the Ungava and Hudson Bay rivers having the highest proportion of filtered REEs (60 and 67%), followed by rivers draining the north (36 ± 20%) and south (11 ± 10%) shores of the St. Lawrence River ( $p < 0.05$ ) (Fig. S1†). The multiple linear regression model showed that lower pH and lower water temperature were the strongest predictors of the

proportion of filtered REEs ( $R^2 = 0.58$ ,  $p < 0.02$ ) (Table S5†), possibly reflecting their influence on REE solubility and particle sorption. Since rivers draining north and south of the St. Lawrence River have similar pH and temperature, differences in geology could help explain the remaining variation in REE concentrations. Notably, northern rivers drain the Canadian Shield, a region naturally enriched in REEs, whereas southern rivers drain the Appalachian region, which is comparatively poorer in REEs.

By contrast to filtered concentrations, there was no significant difference in total  $[REEs]$  among the watersheds ( $p > 0.05$ ) (Fig. 2). However, two highly eroded rivers draining the south shore of the St. Lawrence stood out, namely the Boyer River ( $[REEs] = 27.42 \mu\text{g L}^{-1}$ ) and the Nicolet River ( $[REEs] = 13.09 \mu\text{g L}^{-1}$ ), possibly highlighting the influence of erosion from agricultural activities on REE mobilization to rivers.<sup>21</sup>

### Water chemistry driving REE concentrations and composition across regions

The Principal Component Analysis (PCA) performed on the filtered dataset shows that rivers from the Hudson Bay watershed were colder, higher in DOC concentrations and lower in pH, which corresponded to higher trace metal concentrations in solution (REEs, Fe and Mn; Fig. 3 and 4). Conversely, rivers from the St. Lawrence River watershed displayed higher pH and temperature and lower concentrations of DOC and metals (Fig. 3 and 4). Located further north, rivers draining the Ungava Bay watershed, characterized by permafrost and colder climates, also displayed low concentrations of DOC and metals.

A multiple linear regression model indicated that filtered  $[REEs]$  were best predicted with a combination of DOC and pH ( $R^2 = 0.74$ ,  $p < 0.01$ ; Table S4†). Higher temperature showed lower REEs, but temperature was not a significant predictor in

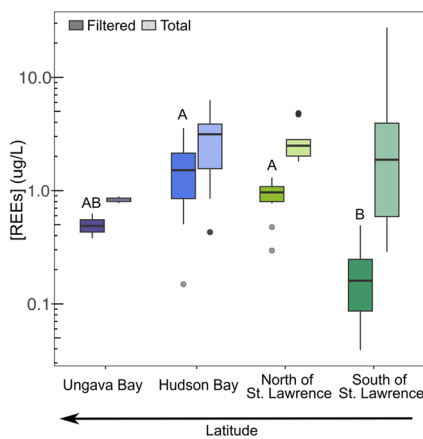


Fig. 2 Filtered (left) and total (right) concentrations of the sum of rare earth elements (REEs) in rivers draining different watersheds from the Province of Québec: the Ungava Bay ( $n = 2$ ), the Hudson Bay ( $n = 18$ ), the north of the St. Lawrence River ( $n = 8$ ) and the south of the St. Lawrence River ( $n = 12$ ). Significant differences ( $p < 0.05$ ) in filtered concentrations are marked by different letters.

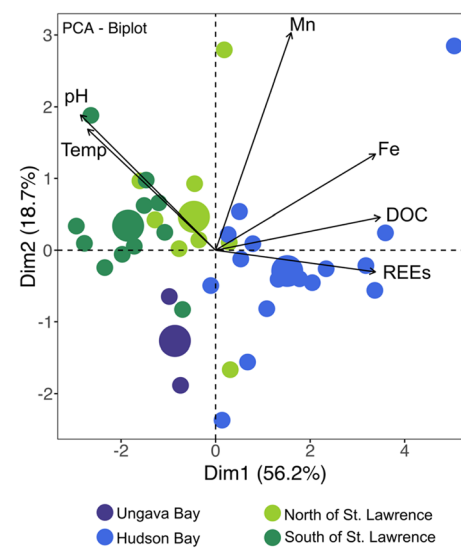


Fig. 3 Principal component analysis in type 2 framing with filtered concentrations of elements in rivers draining the different watersheds of the Province of Québec. Larger circles represent the center of each group distribution.



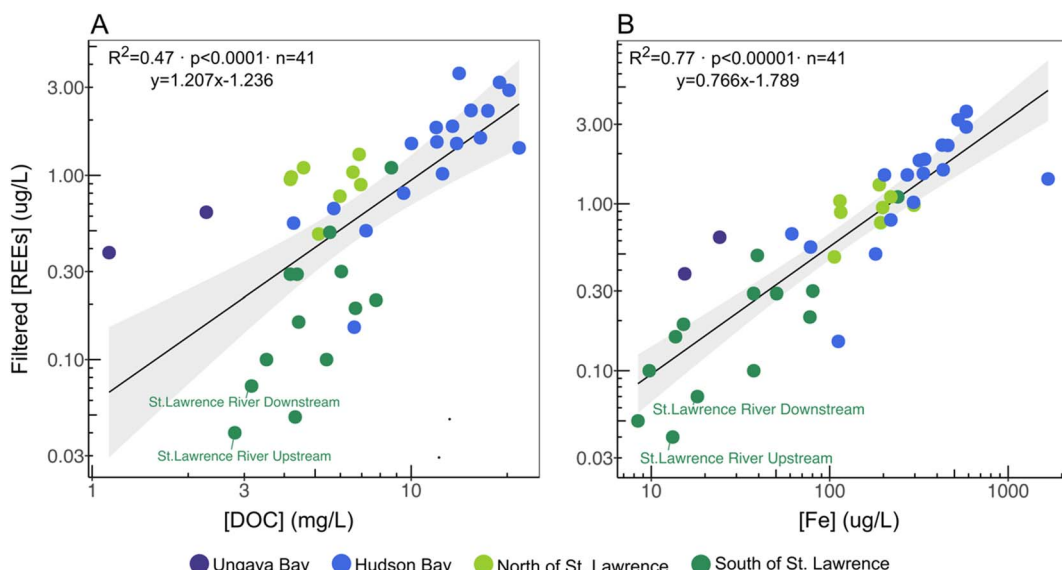


Fig. 4 Filtered concentrations of the sum of rare earth elements (REEs) as a function of (A) dissolved organic matter (DOC) and (B) dissolved iron (Fe) concentrations in rivers draining different watersheds of the Province of Québec. The St. Lawrence River is present twice and identified to highlight upstream downstream differences in concentrations.

this model. While total [REEs] were seemingly controlled by the concentrations of suspended particles (Fig. S2†), they correlated strongly with [Fe] and [Al] and to a lesser extent with [Mn] (Fig. 5). Rivers draining the south shore of the St. Lawrence River followed a distinctive trend compared to other groups. The correlation strength with these controlling factors increased significantly when considering this group alone, denoting the sedimentary geology of the Appalachian region, which is naturally poor in REEs, Fe, and Al (Fig. 5). Overall, these results highlight the combined influence of water chemistry and geology on REE concentrations in rivers from contrasting watersheds and climate zones.

The standardized composition of filtered REEs followed a similar latitudinal gradient to their concentrations (Fig. 6). In rivers draining the agricultural and REE-poor regions of the St. Lawrence Lowlands platform and the Appalachian region, we observed a consistent fractionation characterized by an enrichment in heavier REEs (HREEs). Conversely, rivers draining the Canadian Shield exhibited a fractionation increasingly enriched in light REEs (LREEs) as they progressed northward. This enrichment in LREEs seemed to increase with lower pH ( $R^2 = 0.52$ ,  $p < 0.0001$ ) (Fig. S3†). The Salmon River from the Hudson Bay watershed has the lowest concentrations, which likely reflects the suspected influence of marine water in this

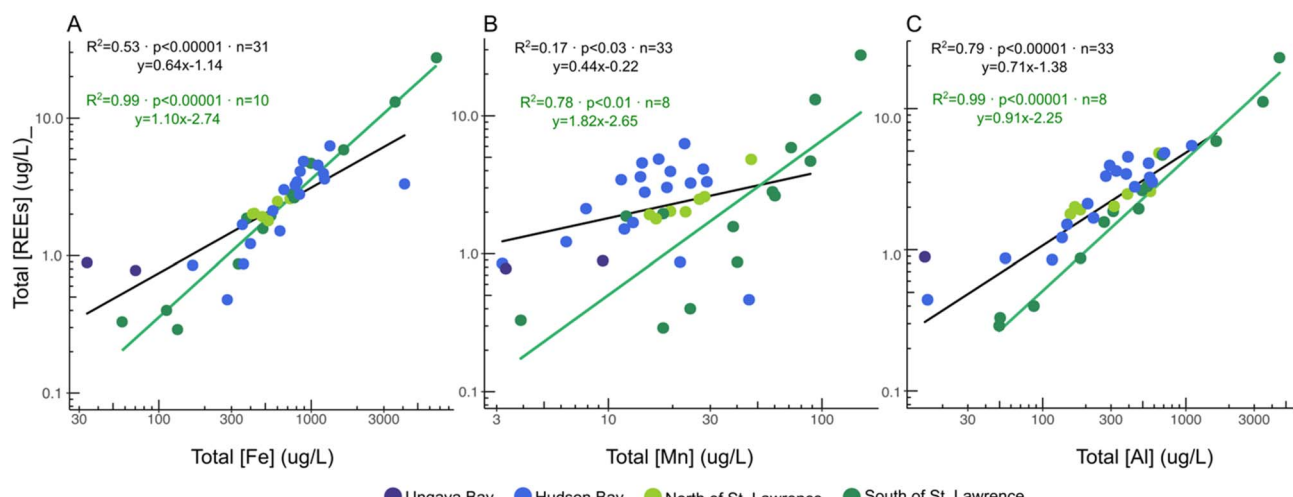
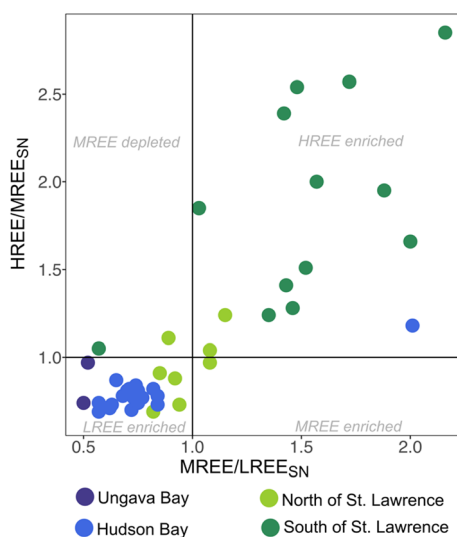


Fig. 5 Total concentrations of the sum of rare earth elements (REEs) as a function of (A) iron (Fe), (B) manganese, and (C) aluminum (Al) concentrations in rivers draining different watersheds of the Province of Québec. The regression line in black includes data for all watersheds with the exception of the rivers draining south of the St. Lawrence River, represented in green.





**Fig. 6** Filtered standardized patterns of rare earth elements (REEs) in rivers draining the different watersheds of the Province of Québec. Light REEs (LREEs) consisted of the sum of shale-normalized (SN) concentrations of La, Pr, and Nd, while middle REEs (MREEs) consisted of the sum of Sm, Gd, and Tb and heavy REEs (HREEs) including Er, Yb and Lu. In the case the sample presented a Gd anomaly, Dy was used instead. The center of the line represents no distinctive deviation from the flat natural pattern of REEs and each quadrant represents a relative enrichment of one of the REE subgroups (LREEs, MREEs, and HREEs) as written in pale grey.

shallow river, also supported by increased specific conductivity ( $896 \mu\text{S cm}^{-1}$ ) and cation concentrations (Table S1†).

### Variation in REE fluxes and yields

Based on river mean runoff and total watershed area located in the Quebec province, we estimated that rivers exported approximately 1078 and 2941 metric tons of REEs per year into the Hudson Bay and the Atlantic Ocean, respectively. Fluxes varied according to river discharge, with the highest total flux reaching  $740 \pm 193$  tons per year in the St. Lawrence River ( $12\ 564 \text{ m}^3 \text{ s}^{-1}$ ), including combined inputs from its tributaries, such as the Ottawa River, which has the second-largest estimated flux at  $137 \pm 19$  tons per year (Table S6† and Fig. 7). When summed together, fluxes from the 18 sampled tributaries of the St. Lawrence River and Lake Ontario outlet equal about half (345 tons per year) of the estimated flux downstream of the St. Lawrence, suggesting other major sources of REEs in this system. The other most important fluxes were the Nottaway River ( $111 \pm 45$  tons per year) and La Grande River ( $84 \pm 35$  tons per year) draining the Hudson Bay watershed. While the La Grande River had the second largest discharge among the studied rivers, it also drains the largest reservoir in Canada ( $4318 \text{ km}^2$ ) and has other important dams upstream, thereby influencing water retention and settling of particles. This may reduce REE concentrations downstream, as indicated by significantly lower yields of total REEs (average =  $1.11 \pm 0.72 \text{ kg km}^2 \text{ year}^{-1}$ ) in dammed rivers compared to undammed ones (average =  $3.34 \pm 5.73 \text{ kg km}^2 \text{ year}^{-1}$ ) ( $p = 0.04$ ) (Fig. S5†).

While the filtered REE fluxes in the Nottaway, Ottawa, and La Grande rivers aligned with discharge, the St. Lawrence River ranked only fifth, similar to the St. Maurice River, despite its discharge being nearly 20 times higher (Fig. 7a). A decrease in filtered REE concentrations and fluxes is even observed along the St. Lawrence, likely reflecting REE sorption on particles and settling (Fig. 4 and 7a). Generally, rivers draining the Hudson Bay watershed ( $0.63 \pm 0.33 \text{ kg km}^2 \text{ year}^{-1}$ ) and north of the St. Lawrence River ( $0.51 \pm 0.20 \text{ kg km}^2 \text{ year}^{-1}$ ) had higher yields of filtered REEs than rivers draining south of the St. Lawrence River ( $0.33 \pm 0.61 \text{ kg km}^2 \text{ year}^{-1}$ ) or the Ungava Bay ( $0.32 \pm 0.11 \text{ kg km}^2 \text{ year}^{-1}$ ), reflecting the combined influence of geology and water chemistry (Fig. 7b and S6†).

Considering anthropogenic influences, the largest yields of total REEs were measured in highly eroded tributaries draining the agricultural south shores of the St. Lawrence River, such as the Saint-Régis ( $20.7 \text{ kg km}^2 \text{ year}^{-1}$ ), Boyer ( $17.7 \text{ kg km}^2 \text{ year}^{-1}$ ) and Nicolet rivers ( $4.0 \text{ kg km}^2 \text{ year}^{-1}$ ) (Table S6† and Fig. 7b). In addition, only rivers draining south of the St. Lawrence River ( $n = 7$ ) exported anthropogenic gadolinium downstream ( $\text{Gd}_{\text{ant}} = 0.2$  to  $134 \text{ kg year}^{-1}$ ) (Fig. S4†). Regardless of its small discharge and watershed, the St. Régis River had the highest flux of anthropogenic Gd ( $\text{Gd}_{\text{ant}} = 133.8 \text{ kg km}^2 \text{ year}^{-1}$ ;  $\text{yield}_{\text{Gd}} = 1.44 \text{ kg km}^2 \text{ year}^{-1}$ ), which contributed to 98% and 67% of its filtered and total Gd fluxes, respectively. The other anthropogenic fluxes contributed between 13 and 55% of the filtered Gd exported by these rivers. However, we did not measure any anomaly or anthropogenic concentrations of Gd downstream of the St. Lawrence River, implying that this anthropogenic Gd entering the St. Lawrence, as well as the one rejected by Montreal wastewater effluent,<sup>21</sup> is diluted or potentially lost to sediments.

### Discussion

In this study, we provided a comprehensive estimate of rare earth element (REE) fluxes over 40 widely distributed rivers in Quebec, Canada, and we extrapolated REE fluxes to the whole  $1\ 496\ 000 \text{ km}^2$  of Quebec territory. We estimated that the Province of Quebec exports annually a total of 1078 and 2941 metric tons of REEs towards the two main receiving marine ecosystems, the Hudson Bay and the Atlantic Ocean, respectively. As expected, rivers with the highest discharge contributed the most significantly to the total REE fluxes, but the proportion exported in their filtered form and their relative composition varied regionally, which was attributed to influences of water quality (DOC, pH, temperature, and Fe). Furthermore, some of the rivers flowing through densely populated regions exported anthropogenic gadolinium (Gd) downstream, contributing significantly to their overall filtered Gd flux. These findings establish baseline REE fluxes and drivers for the entire Province of Quebec, crucial for predicting or assessing the regional impacts of the evolution of anthropogenic activities<sup>64,65</sup> or of climate change factors,<sup>66</sup> including temperature rise, permafrost thaw, ice and snow melt, precipitation variations, and



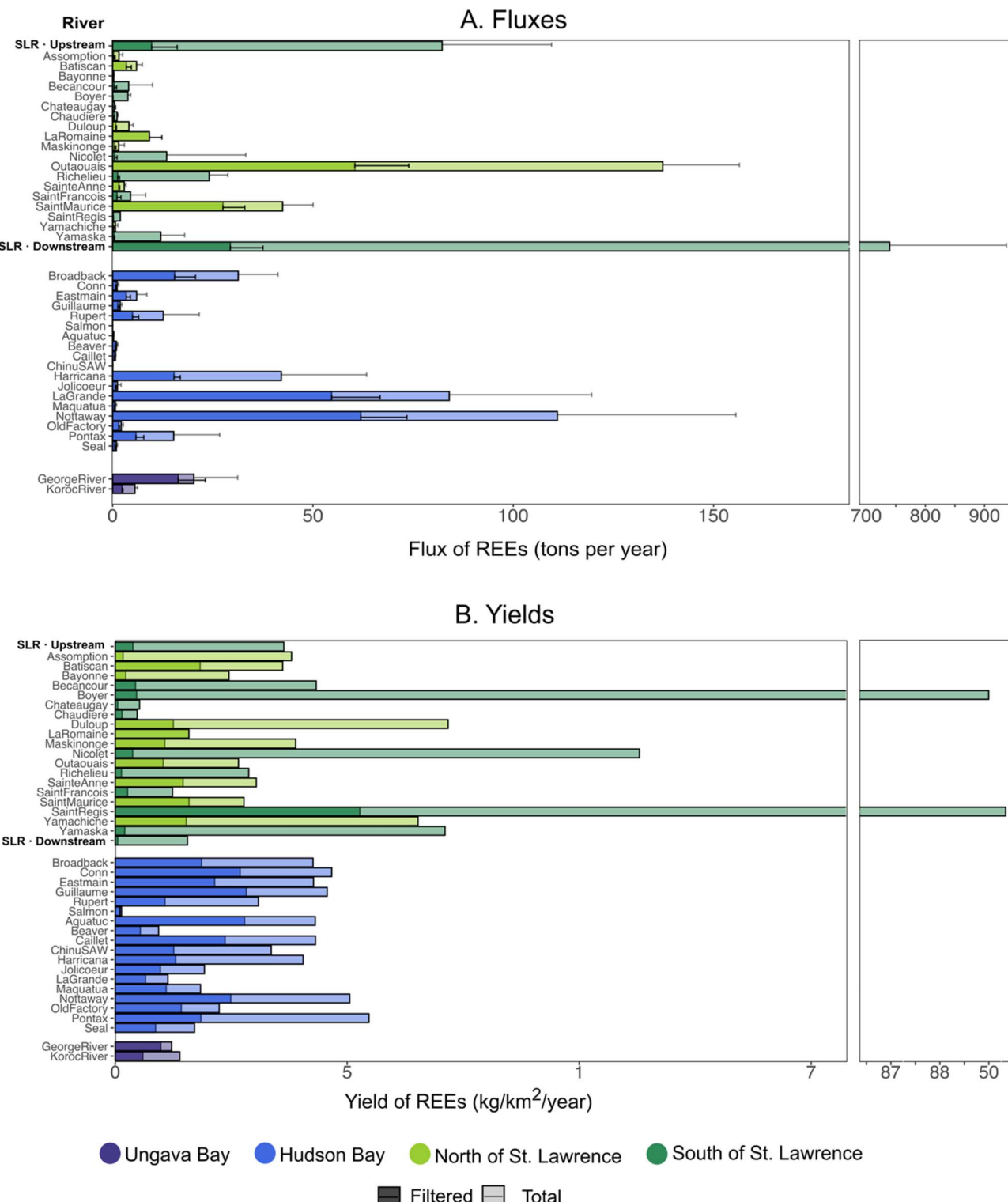


Fig. 7 Fluxes (A) and yields (B) of filtered and total rare earth elements (REEs) in the rivers from the different watersheds of the Province of Québec. Error bars are standard deviations. The St. Lawrence River (in bold) is represented twice, so we can see differences between the upstream and downstream sites.

increased carbon mobilization. Moreover, the patterns and their drivers reported below presumably transpose well to other northern landscapes around the globe.

#### Regional drivers of rare earth element concentrations

From a large-scale perspective, concentrations of REEs varied latitudinally, likely due to contrasting geology and climate



affecting water chemistry. Rivers located south of the St. Lawrence River drain Ordovician limestones from the Appalachian region and the St. Lawrence Lowlands where bedrock is naturally poor in REEs (SIGÉOM).<sup>36</sup> This is reflected in their lower filtered concentrations when compared to rivers mainly draining the boreal forest of the Canadian Shield, naturally rich in DOC and REEs<sup>65</sup> (Fig. 2). As expected, pH and DOC were the best predictors of the filtered concentrations of REEs.<sup>21</sup> Rivers draining the granitic soils of the Canadian Shield typically exhibit low ionic strength, which enhances the solubility of DOC and increases its reactivity with metals, potentially influencing their mobility and bioavailability.<sup>29,67</sup> Due to their abundance in functional groups rich in oxygen such as carboxylic or phenolic sites, humic- and fulvic-like dissolved organic matter (DOM) are dominant transporters of dissolved REEs in freshwater ecosystems, as opposed to proteinic-like DOC.<sup>20,21,68,69</sup> The increased mobilization of terrestrial carbon expected with more abundant and frequent precipitations, river and lake browning, and thawing of permafrost in Northern Quebec<sup>14</sup> could therefore enhance REE fluxes into marine ecosystems.

Conditions promoting higher proportions and concentrations of REEs in solution may account for the increasing relative enrichment of filtered LREEs with latitude within the main watersheds (Fig. 6 and S3†). As discussed by Marginson and MacMillan,<sup>38</sup> due to their enhanced adsorption onto Fe- and Mn-rich colloids or particles under alkaline conditions, LREEs are more stable in solutions of slightly acidic rivers, such as those in the Hudson Bay watershed<sup>19,32,70</sup> (Fig. 4b). Alternatively, an enrichment of LREEs in the filtered fraction  $<0.45\text{ }\mu\text{m}$  is commonly attributed to the effect of colloids passing through this filter size.<sup>29</sup> However, this explanation does not account for the northward gradient or the contrast with the rivers draining the St. Lawrence Lowlands and the Appalachian region. Nevertheless, within the total fraction, REE transport would predominantly be controlled by colloids and particles of Fe and Mn oxyhydroxides, along with mineral particles rich in Al, especially for rivers from the St. Lawrence River watershed having higher amounts of particles (Fig. 5). These minerals have large specific surface areas, so they are very effective at binding REEs in aquatic systems through adsorption, surface precipitation, oxidation, and scavenging processes.<sup>71-73</sup> It is also possible that during the summer, the prolonged solar exposure of surface water in rivers located at higher latitudes contributes to increased photoreduction of particles sensitive to redox reactions, particularly in the presence of DOM.<sup>74</sup> This process could also alter the speciation and the mobility of associated metals, which could promote their release to surface waters, thereby enriching LREEs in the filtered phase.<sup>75</sup> In addition to the effect of pH on oxyhydroxide particles, water temperature played a significant role in predicting the proportion of the filtered REEs in sampled rivers. When tested, these variables showed a moderate positive correlation ( $R^2 = 0.58$ ), so their effects on REEs are partly related. Rivers from the St. Lawrence River watershed, characterized by a cold and humid continental climate, displayed warmer surface water temperature at the time of sampling ( $18.7 \pm 3.6\text{ }^\circ\text{C}$ ) than rivers draining the

Hudson Bay, including the Ungava Bay, characterized by a subpolar continental climate ( $13.5 \pm 3.2\text{ }^\circ\text{C}$ ). These few degrees of difference could influence the solubility of dissolved REEs, as has been shown across various northern aquatic environments spanning a broader temperature range (2.4–19.5  $^\circ\text{C}$ ).<sup>38</sup> In warmer waters, lower  $\text{CO}_2$  levels cause a shift in the carbonate equilibrium, reducing the availability of carbonate ions that typically form complexes with dissolved REEs. As a result, colder waters, with higher  $\text{CO}_2$ , more available carbonates and lower pH, may enhance the solubility of REEs, particularly light REEs (LREEs), which are generally less soluble compared to heavy REEs (HREEs). Overall, these findings indicate that geology and climate exert an important large-scale control on the water chemistry influencing REE concentrations and composition in temperate and boreal rivers within the Quebec province.

### REE fluxes and yields

Fluxes and yields of REEs in the Quebec province varied according to geology, discharge, and anthropogenic influence. Large rivers located in the Atlantic watershed and characterized by significant particle export, such as the St. Lawrence River and the Ottawa River, had a prominent role in exporting total REEs towards marine ecosystems (Fig. 7). Although total REE concentrations did not vary significantly between main watersheds (Fig. 1), rivers draining the boreal forest and the REE-rich area of the Canadian Shield exported more filtered REEs per  $\text{km}^2$  than rivers draining the agricultural plains and the REE-poor area of the St. Lawrence Lowlands and Appalachian region (Fig. 7 and S6†). While filtered REE fluxes measured downstream of the St. Lawrence River represented less than 4% of the total exported REEs, over 35% of the total flux appeared to originate from particle sources other than its main tributaries (~65% contribution), likely due to sediment resuspension or in-river erosion. For example, in the Brazilian Ipojuca River, more than 95% of downstream REE fluxes were attributed to resuspended sediments<sup>72</sup> and similar patterns have been reported in other large river systems worldwide.<sup>76</sup> In a mass balance budget study, Rondeau<sup>77</sup> estimated that St. Lawrence tributaries accounted for approximately 32% of the suspended sediment load measured downstream, while the erosion of the beds and banks of the St. Lawrence River accounted for 65%. Given that the St. Lawrence River lies on a REE-poor geological formation, the significant contribution from resuspended sediments may seem counterintuitive. However, this likely reflects the remobilization of REE-enriched particles previously deposited from upstream tributaries draining the Canadian Shield, a region naturally rich in REEs. Sedimentation zones along the river act as transient sinks, where REEs accumulate over time before being resuspended and exported downstream during high-flow events or through bed and bank erosion.

While fluxes, which are mostly driven by discharge, provide a broad portrait of the average watershed properties across broad spatial extents, yields provide additional insights into the identification of hotspots, the importance of geological or anthropogenic influence and the potential temporal trends



(Table S5† and Fig. 7b). Studies reporting the total flux and yield of the sum of REEs are scarce, but dissolved neodymium (Nd) fluxes have been more widely reported, due to the information its isotopes reveal about past and present ocean circulation and land erosion dynamics.<sup>8,18,78</sup> The yields of filtered Nd (<0.45 µm) observed in this study, including the St. Lawrence River (0.06 kg km<sup>-2</sup> year<sup>-1</sup>), were lower than those of dissolved Nd (<0.22 µm) estimated in other large rivers within sub-equatorial to tropical climates, such as the Orinoco River (0.34 kg km<sup>-2</sup> year<sup>-1</sup>),<sup>17</sup> the Congo River (0.16 kg km<sup>-2</sup> year<sup>-1</sup>),<sup>8</sup> and the Amazon River (0.09–0.80 kg km<sup>-2</sup> year<sup>-1</sup>).<sup>18,78</sup> Consequently, the Quebec river contribution to the global Atlantic dissolved flux would be much less significant globally, especially considering the larger colloids included in our filtered fraction (0.45 vs. 0.22 µm). However, while REEs are primarily partitioned into the particulate phase, total fluxes and yields of REEs are lacking, which limits accurate global comparisons of river contributions and specific ecosystem inputs.

Human activities can influence both the quantity and composition of rare earth elements (REEs) exported downstream, sometimes independent of water flow. This variability could complicate future predictions of fluxes and yields. Hydroelectric dams and reservoirs alter element cycling and fluxes in rivers by flooding large soil areas, increasing water depth and retention time, and reducing flow velocity, which promotes particle settling.<sup>39,79</sup> This explains the lower REE yields in dammed rivers compared to undammed ones, as REEs primarily adsorb onto organic matter and particles<sup>21,68,80</sup> (Fig. S5†). Similar trends are observed for DOC and mercury.<sup>37,39,47</sup> Thus, dammed rivers seemingly act as sinks for REEs, though local food webs may still be affected by potential bioaccumulation.

In addition to dams, several rivers located south of Quebec province, draining REE-poor geological areas, were heavily impacted by agricultural activities and emerged as hotspots for total REE export (Fig. 7b). Notable examples include the St. Regis, Boyer, and Nicolet rivers, where agricultural land use accounts for 71%, 66%, and 44% of their respective watersheds.<sup>35</sup> The Boyer River, receiving untreated domestic wastewater, even displayed a positive anomaly of filtered praseodymium (Pr/Pr\* = 3.8), of unknown origin, supporting the influence of human activities on the export of specific REEs. Moreover, seven rivers from this area displayed a positive anomaly of filtered gadolinium (Gd), typically associated with wastewater containing Gd-based contrast agents used in medical magnetic resonance imaging (MRI) procedures (Fig. S4†).<sup>3,25,81</sup> With the exception of the St. Regis river exporting almost exclusively anthropogenic Gd downstream (98%), the rivers exhibited similar anthropogenic contributions to dissolved Gd fluxes and yields to values reported for the Garonne River (22–60%; 0.001 kg km<sup>-2</sup> year<sup>-1</sup>) by Lerat-Hardy and Coyne<sup>2</sup> (Table S5†). As argued in this study, with the aging population and the increased incidence of global cancers and neurodegenerative diseases, the medical need for MRIs is predicted to increase, as are the fluxes of anthropogenic gadolinium. Evaluating the long-term yields of Gd in these rivers is therefore crucial for monitoring its evolution and for targeting

areas to focus waste reduction efforts. Although no anthropogenic anomalies have been identified further downstream of the St. Lawrence River (Gd/Gd\* < 1.4), these findings suggest the significant impact of human activities on the magnitude and composition of REE fluxes at the local scale.

Although total REE yields were not significantly different across major watersheds (Fig. S6†), it is notable that rivers south of the St. Lawrence River, despite draining soils naturally low in REEs and dissolved organic carbon (DOC), exhibited yields comparable to those of boreal forest rivers, where REE-rich soils are more common. Intensive erosion in agricultural tributaries and specific farming practices (e.g., the application of phosphate fertilizers or type of agricultural crops) may significantly enhance the availability and transport of REEs from these areas to surrounding water systems.<sup>21,80</sup> According to Sen and Peucker-Ehrenbrink,<sup>28</sup> uncertainties in quantifying the human contribution to soil erosion hinder the attribution of REE fluxes to natural or anthropogenic sources. Yet, their assessment shows that neglecting human-driven erosion limits the estimated anthropogenic share of REE fluxes to ~10%, whereas accounting for a 50% contribution raises it to over 45%, revealing the extent to which erosion-related inputs may be overlooked. Therefore, while some anthropogenic sources of REEs, such as industrial effluents, are readily identifiable, diffuse processes such as erosion remain underestimated and require greater attention to accurately quantify human contributions to REE fluxes. However, our comprehensive assessment of REE fluxes and anomalies offers a critical baseline for detecting future changes driven by expanding REE exploitation and broader land-use transformations.

From a broader perspective, alongside increasing erosion and increasing anthropogenic emissions, the anticipated effects of climate change in Northern Quebec, such as heightened precipitation, permafrost thaw, and browning of aquatic systems, are likely to intensify the mobilization of rare REEs in the region. These changes will result in higher concentrations of terrestrial dissolved organic carbon,<sup>14,66</sup> which can enhance the transport of REEs to aquatic systems.<sup>21,30,38</sup> As these dynamics evolve, the impact on downstream ecosystems will likely become more pronounced, necessitating ongoing monitoring and adaptive management strategies. Consequently, the contribution of total REEs exported from this area could significantly increase in the coming years, driven by both natural and human-induced factors.

## Conclusions

In summary, this study sheds light on the dynamics and significance of both filtered and total REE fluxes across diverse temperate, boreal, and subarctic ecosystems, offering valuable insights into the global biogeochemical cycle of REEs. It also provides critical information for monitoring REE exports from Canadian watersheds, which is essential for guiding environmental protection efforts and assessing the potential impacts of new mining or industrial activities. Moreover, by identifying key factors influencing REE fluxes, composition, and speciation—such as DOC, pH, temperature, and geology—this study enables



the prediction of increased REE exports in the coming years, driven by climate change-induced mobilization of terrestrial carbon into northern aquatic ecosystems. In addition to estimating total REE fluxes for rivers from multiple regions of the world, future research could prioritize investigating their coupling with terrestrial organic matter, particularly in response to long-term and seasonal shifts in northern ecosystems, and the relative impact of the increasing anthropogenic activities, including changes in land use, associated erosion and REE mining.

## Data availability

Data for this article, including physicochemical data, REE concentrations, fluxes and yields are available through project metaGRIL, hosted on Borealis, The Canadian Dataverse Repository, at <https://doi.org/10.5683/SP3/E0A6SF>.

## Author contributions

Marie-Christine Lafrenière: conceptualization, methodology, software, formal analysis, investigation, data curation, writing – original draft, writing – review and editing, visualization. Md Samrat Alam: conceptualization, writing – review and editing, data curation. Jean-François Lapierre: conceptualization, supervision, writing – review and editing, project administration. Dominic E. Ponton: methodology, writing – review and editing, data curation. Maxime Wauthy: conceptualization, methodology, writing – review and editing. Caroline Fink-Mercier: investigation, writing – review and editing. Holly Marginson: investigation, writing – review and editing, visualization. Paul del Gorgio: resources, writing – review and editing, funding acquisition. Marc Amyot: conceptualization, resources, writing – review and editing, supervision, project administration, funding acquisition.

## Conflicts of interest

There are no conflicts to declare.

## Acknowledgements

We thank Maria Chrifi-Alaoui and Dominic Bélanger for continuous help in the lab and support. We thank everyone involved in the collection of samples, including Gwyneth Ann Macmillan for data collection in the George and Koroc rivers. We thank Réseau Quebec Maritime and the people included in the fieldwork on the Lampsilis research vessel from Université du Québec à Trois-Rivières from 2017 to 2020. We also thank Hydro-Québec, Ouranos, Bassin-Versant Saint-Maurice, and the Niskamoon Corporation members, as well as the Innus (La Romaine), the Atikamekw (Haute-Mauricie), the Cree (James Bay) and the Inuit (George River and Koroc River) land users, for their precious partnership, in granting us access to their ancestral lands and their guidance in the field. Funding was provided by the Northern Contaminant Program of Indigenous and Northern Affairs Canada, an NSERC strategic grant

(TRIVALENCE; MA), NSERC Alliance grants (TAMTEC, ARCMITE) and the Canada Research Chair Program (MA). MCL received an FQRNT scholarship (<https://doi.org/10.69777/302608>) and financial support from the FRQNT strategic network GRIL (GRIL-PCR-20H02: <https://doi.org/10.69777/341034>).

## References

- V. Hatje, K. W. Bruland and A. R. Flegal, Increases in Anthropogenic Gadolinium Anomalies and Rare Earth Element Concentrations in San Francisco Bay over a 20 Year Record, *J. Environ. Sci. Technol.*, 2016, **50**(8), 4159–4168.
- A. Lerat-Hardy, A. Coynel, L. Dutruch, C. Pereto, C. Bossy, T. Gil-Diaz, *et al.*, Rare Earth Element fluxes over 15 years into a major European Estuary (Garonne-Gironde, SW France): hospital effluents as a source of increasing gadolinium anomalies, *Sci. Total Environ.*, 2019, **656**, 409–420.
- S. Kulaksiz and M. Bau, Anthropogenic dissolved and colloid/nanoparticle-bound samarium, lanthanum and gadolinium in the Rhine River and the impending destruction of the natural rare earth element distribution in rivers, *Earth Planet. Sci. Lett.*, 2013, **362**, 43.
- N. Malhotra, H.-S. Hsu, S.-T. Liang, M. J. M. Roldan, J.-S. Lee, T.-R. Ger, *et al.*, An updated review of toxicity effect of the rare earth elements (REEs) on aquatic organisms, *Animals*, 2020, **10**(9), 1663.
- M. Trifuggi, G. Pagano, M. Guida, A. Palumbo, A. Siciliano, M. Gravina, *et al.*, Comparative toxicity of seven rare earth elements in sea urchin early life stages, *Environ. Sci. Pollut. Res.*, 2017, **24**, 20803–20810.
- I. Blinova, A. Lukjanova, M. Muna, H. Vija and A. Kahru, Evaluation of the potential hazard of lanthanides to freshwater microcrustaceans, *Sci. Total Environ.*, 2018, **642**, 1100–1107.
- B. S. Cui, Q. J. Zhang, K. J. Zhang, X. H. Liu and H. G. Zhang, Analyzing trophic transfer of heavy metals for food webs in the newly-formed wetlands of the Yellow River Delta, China, *Environ. Pollut.*, 2011, **159**(5), 1297.
- P. Rahlf, G. Laukert, E. C. Hathorne, L. H. Vieira and M. Frank, Dissolved neodymium and hafnium isotopes and rare earth elements in the Congo River Plume: tracing and quantifying continental inputs into the southeast Atlantic, *Geochim. Cosmochim. Acta*, 2021, **294**, 192–214.
- C. Jeandel, J. Bishop and A. Zindler, Exchange of neodymium and its isotopes between seawater and small and large particles in the Sargasso Sea, *Geochim. Cosmochim. Acta*, 1995, **59**(3), 535–547.
- T. C. C. Rousseau, J. E. Sonke, J. Chmeleff, P. van Beek, M. Souhaut, G. Boaventura, *et al.*, Rapid neodymium release to marine waters from lithogenic sediments in the Amazon estuary, *Nat. Commun.*, 2015, **6**(1), 7592.
- E. Sholkovitz, H. Elderfield, R. Szymczak and K. Casey, Island weathering: river sources of rare earth elements to the Western Pacific Ocean, *Mar. Chem.*, 1999, **68**(1–2), 39–57.



12 K. Tachikawa, V. Athias and C. Jeandel, Neodymium budget in the modern ocean and paleo-oceanographic implications, *J. Geophys. Res.:Oceans*, 2003, **108**(C8), 3254.

13 M. G. Novak, A. Mannino, J. B. Clark, P. Hernes, M. Tzortziou, R. G. Spencer, *et al.*, Arctic biogeochemical and optical properties of dissolved organic matter across river to sea gradients, *Front. Mar. Sci.*, 2022, **9**, 949034.

14 M. Wauthy, M. Rautio, K. S. Christoffersen, L. Forsström, I. Laurion, H. L. Mariash, *et al.*, Increasing dominance of terrigenous organic matter in circumpolar freshwaters due to permafrost thaw, *Limnol. Oceanogr. Lett.*, 2018, **3**(3), 186–198.

15 T. Arsouze, J.-C. Dutay, F. Lacan and C. Jeandel, Reconstructing the Nd oceanic cycle using a coupled dynamical-biogeochemical model, *Biogeosciences*, 2009, **6**(12), 2829–2846.

16 V. Hatje, J. Schijf, K. H. Johannesson, R. Andrade, M. Caetano, P. Brito, *et al.*, The Global Biogeochemical Cycle of the Rare Earth Elements, *Global Biogeochem. Cycles*, 2024, **38**(6), e2024GB008125.

17 A. Mora, C. Moreau, J.-S. Moquet, M. Gallay, J. Mahlknecht and A. Laraque, Hydrological control, fractionation, and fluxes of dissolved rare earth elements in the lower Orinoco River, Venezuela, *Appl. Geochem.*, 2020, **112**, 104462.

18 G. Barroux, J. E. Sonke, G. Boaventura, J. Viers, Y. Godderis, M.-P. Bonnet, *et al.*, Seasonal dissolved rare earth element dynamics of the Amazon River main stem, its tributaries, and the Curuá floodplain, *Geochem., Geophys., Geosyst.*, 2006, **7**(12), Q12005.

19 E. R. Sholkovitz, The aquatic chemistry of rare earth elements in rivers and estuaries, *Appl. Geochem.*, 1995, **1**(1), 1–34.

20 K. Andersson, R. Dahlqvist, D. Turner, B. Stolpe, T. Larsson, J. Ingri, *et al.*, Colloidal rare earth elements in a boreal river: changing sources and distributions during the spring flood, *Geochim. Cosmochim. Acta*, 2006, **70**(13), 3261–3274.

21 M.-C. Lafrenière, J.-F. Lapierre, D. E. Ponton, F. Guillemette and M. Amyot, Rare earth elements (REEs) behavior in a large river across a geological and anthropogenic gradient, *Geochim. Cosmochim. Acta*, 2023, **353**, 129–141.

22 A. N. Abbott, B. A. Haley, J. McManus and C. E. Reimers, The sedimentary flux of dissolved rare earth elements to the ocean, *Geochim. Cosmochim. Acta*, 2015, **154**, 186–200.

23 M. I. Leybourne and K. H. Johannesson, Rare earth elements (REE) and yttrium in stream waters, stream sediments, and Fe–Mn oxyhydroxides: fractionation, speciation, and controls over REE+Y patterns in the surface environment, *Geochim. Cosmochim. Acta*, 2008, **72**(24), 5962–5983.

24 R. H. Byrne and K.-H. Kim, Rare earth element scavenging in seawater, *Geochim. Cosmochim. Acta*, 1990, **54**(10), 2645–2656.

25 M. Bau, A. Knappe and P. Dulski, Anthropogenic gadolinium as a micropollutant in river waters in Pennsylvania and in Lake Erie, northeastern United States, *Geochemistry*, 2006, **66**(2), 143–152.

26 S. Kulaksiz and M. Bau, Rare earth elements in the Rhine River, Germany: first case of anthropogenic lanthanum as a dissolved microcontaminant in the hydrosphere, *Environ. Int.*, 2011, **37**(5), 973.

27 Y. Zhu, M. Hoshino, H. Yamada, A. Itoh and H. Haraguchi, Gadolinium Anomaly in the Distributions of Rare Earth Elements Observed for Coastal Seawater and River Waters around Nagoya City, *Bull. Chem. Soc. Jpn.*, 2004, **77**(10), 1835–1842.

28 I. S. Sen and B. Peucker-Ehrenbrink, Anthropogenic Disturbance of Element Cycles at the Earth's Surface, *Environ. Sci. Technol.*, 2012, **46**(16), 8601–8609.

29 J. Ingri, A. Widerlund, M. Land, Ö. Gustafsson, P. Andersson and B. Öhlander, Temporal variations in the fractionation of the rare earth elements in a boreal river; the role of colloidal particles, *Chem. Geol.*, 2000, **166**(1), 23–45.

30 B. Stolpe, L. Guo and A. M. Shiller, Binding and transport of rare earth elements by organic and iron-rich nanocolloids in Alaskan rivers, as revealed by field-flow fractionation and ICP-MS, *Geochim. Cosmochim. Acta*, 2013, **106**, 446–462.

31 B. Dupré, J. Viers, J.-L. Dandurand, M. Polve, P. Bénézeth, P. Vervier, *et al.*, Major and trace elements associated with colloids in organic-rich river waters: ultrafiltration of natural and spiked solutions, *Chem. Geol.*, 1999, **160**(1), 63–80.

32 S. B. Adebayo, M. Cui, T. Hong, C. D. White, E. E. Martin and K. H. Johannesson, Rare Earth Elements Geochemistry and Nd Isotopes in the Mississippi River and Gulf of Mexico Mixing Zone, *Front. Mar. Sci.*, 2018, **5**, 166, DOI: [10.3389/fmars.2018.00166](https://doi.org/10.3389/fmars.2018.00166).

33 Natural Resources Canada, *Rare earth elements facts*, 2021, available from: <https://www.nrcan.gc.ca/our-natural-resources/minerals-mining/minerals-metals-facts/rare-earth-elements-facts/20522>.

34 J.-M. Martin, O. Høgdahl and J. C. Philippot, Rare earth element supply to the Ocean, *J. Geophys. Res.*, 1976, **81**(18), 3119–3124.

35 Gouvernement du Québec, *cartographer Atlas de l'eau: cours d'eau [Multimedia cartography]*, 2021.

36 *Carte interactive géologique et minière du Québec*, Gouvernement du Québec, 2024, available from: [https://sigeom.mines.gouv.qc.ca/signet/classes/I1108\\_afchCarteIntr?l=F&m=B&ll=49.30665,-66.26270&z=5&c=MP\\_ETR%7C100,prov%7C100&op=mspQc%7Call%7C&af=light](https://sigeom.mines.gouv.qc.ca/signet/classes/I1108_afchCarteIntr?l=F&m=B&ll=49.30665,-66.26270&z=5&c=MP_ETR%7C100,prov%7C100&op=mspQc%7Call%7C&af=light).

37 M. Wauthy, M. Amyot, D. E. Ponton, C. Fink-Mercier, F. Bilodeau, A. Tremblay, *et al.*, Riverine exports of mercury and methylmercury from dammed and undammed rivers of Quebec, Eastern Canada. Estuarine, Estuarine, Coastal Shelf Sci., 2023, **284**, 108272.

38 H. Marginson, G. A. MacMillan, M. Wauthy, E. Sicaud, J. Gérin-Lajoie, J. P. Dedieu, *et al.*, Drivers of rare earth elements (REEs) and radionuclides in changing subarctic (Nunavik, Canada) surface waters near a mining project, *J. Hazard. Mater.*, 2024, **471**, 134418.

39 C. Fink-Mercier, J.-F. Lapierre, M. Amyot and P. A. del Giorgio, Concentrations and Yields of Total Hg and MeHg in Large Boreal Rivers Linked to Water and Wetland



Coverage in the Watersheds, *J. Geophys. Res.: Biogeosci.*, 2022, **127**(5), e2022JG006892.

40 J. De Bonville, M. Amyot, P. del Giorgio, A. Tremblay, F. Bilodeau, D. E. Ponton, *et al.*, Mobilization and Transformation of Mercury Across a Dammed Boreal River Are Linked to Carbon Processing and Hydrology, *Water Resour. Res.*, 2020, **56**(10), e2020WR027951.

41 *Atlas hydroclimatique – Stations Hydrométriques*, 2024, available from: <https://www.cehq.gouv.qc.ca/atlas-hydroclimatique/stations-hydrometriques/index.htm>.

42 S. Lachance-Cloutier, R. Turcotte and J.-F. Cyr, Combining streamflow observations and hydrologic simulations for the retrospective estimation of daily streamflow for ungauged rivers in southern Quebec (Canada), *J. Hydrol.*, 2017, **550**, 294–306.

43 *Lake Ontario Outflow Changes*, 2024, available from: <https://ijc.org/en/losrb/watershed/outflow-changes>.

44 *Débit mensuel d'eau douce du Saint-Laurent à la hauteur de la Ville de Québec*, 2023, available from: [https://catalogue.ogsl.ca/dataset/ca-cioos\\_84a17ffc-4898-4261-94de-4a5ea2a9258d?local=fr](https://catalogue.ogsl.ca/dataset/ca-cioos_84a17ffc-4898-4261-94de-4a5ea2a9258d?local=fr).

45 *Freshwater runoffs – Québec City – Application*, 2024, available from: <https://ogsl.ca/en/freshwater-runoffs-quebec-city-application/>.

46 *Ottawa River at Carillon*, 2024, available from: <https://ottawariver.ca/information/historical-water-level-streamflow-summary/ottawa-river-at-carillon/>.

47 M. L. De Melo, M.-L. Gérardin, C. Fink-Mercier and P. A. Del Giorgio, Patterns in riverine carbon, nutrient and suspended solids export to the Eastern James Bay: links to climate, hydrology and landscape, *Biogeochemistry*, 2022, **161**(3), 291–314.

48 I. Jreije, M. Hadioui and K. J. Wilkinson, Sample preparation for the analysis of nanoparticles in natural waters by single particle ICP-MS, *Talanta*, 2022, **238**, 123060.

49 Agilent Technologies, *Direct Measurement of Trace Rare Earth Elements (REEs) in High-Purity RE Oxide Using the Agileent 8800 Triple Quadrupole ICP-MS with MS/MS Mode*, 2012, Contract No.: 5991-0892EN.

50 L. Yang, K. Nadeau, P. Grinberg, C. Brophy, I. Pihillagawa Gedara, J. Meija, *et al.*, SLRS-6: River Water Certified Reference Material for Trace Metals and other Constituents SLRS-6, National Research Council of Canada, 2015.

51 Yeghicheyan D., Aubert D., Bouhnik-Le Coz M. and Chmeleff J., *A New Compilation of Element Concentrations in the Natural River Water Standard SLRS-6 (NRC-CNRC)*. Goldschmidt Conference 2017, 2017.

52 R. C. Antweiler and H. E. Taylor, Evaluation of statistical treatments of left-censored environmental data using coincident uncensored data sets: I. Summary statistics, *Environ. Sci. Technol.*, 2008, **42**(10), 3732–3738.

53 A. Pourmand, N. Dauphas and T. J. Ireland, A novel extraction chromatography and MC-ICP-MS technique for rapid analysis of REE, Sc and Y: Revising CI-chondrite and Post-Archean Australian Shale (PAAS) abundances, *Chem. Geol.*, 2012, **291**, 38–54.

54 J. Rétif, A. Zalouk-Vergnoux, N. Briant and L. Poirier, From geochemistry to ecotoxicology of rare earth elements in aquatic environments: diversity and uses of normalization reference materials and anomaly calculation methods, *Sci. Total Environ.*, 2023, **856**, 158890.

55 C. Hissler, R. Hostache, J. F. Iffly, L. Pfister and P. Stille, Anthropogenic rare earth element fluxes into floodplains: coupling between geochemical monitoring and hydrodynamic sediment transport modelling, *C.R. Geosci.*, 2015, **347**(5), 294–303.

56 M. Rabiet, F. Brissaud, J. L. Seidel, S. Pistre and F. Elbaz-Poulichet, Positive gadolinium anomalies in wastewater treatment plant effluents and aquatic environment in the Hérault watershed (South France), *Chemosphere*, 2009, **75**(8), 1057–1064.

57 R Development Core Team, *R: A Language and Environment for Statistical Computing*, R Foundation for Statistical Computing, 2023.

58 H. Wickham and H. Wickham, *Data Analysis*, Springer, 2016.

59 H. Wickham, R. François, L. Henry, K. Müller and D. Vaughan, *Dplyr: A Grammar of Data Manipulation*, R package version 1.1.4, <https://github.com/tidyverse/dplyr>, <https://dplyr.tidyverse.org.ed2023>.

60 S. Xu, M. Chen, T. Feng, L. Zhan, L. Zhou and G. Yu, Use ggbreak to Effectively Utilize Plotting Space to Deal With Large Datasets and Outliers, *Front. Genet.*, 2021, **12**, DOI: [10.3389/fgene.2021.774846](https://doi.org/10.3389/fgene.2021.774846).

61 S. Lê, J. Josse and F. Husson, FactoMineR: An R Package for Multivariate Analysis, *J. Stat. Software*, 2008, **25**(1), 1–18.

62 J. Fox, G. G. Friendly, S. Graves, R. Heiberger, G. Monette, H. Nilsson, *et al.*, *The Car Package*. R Foundation for Statistical Computing, 2007, vol. 1109, p. , p. 1431.

63 A. Hebbali and M. A. Hebbali, *Package 'olsrr'*, Version 05, 2017, vol. 3.

64 Tornat, *Tornat Metals*, 2024, available from: <https://tornatmetals.com>.

65 Ministère des Ressources Naturelles et des Forêts, *Substances métalliques: Éléments de terres rares*, 2024, available from: <https://gq.mines.gouv.qc.ca/portail-substances-minerales/elements-des-terres-rares/#:~:text=ExploitationauQu%C3%A9bec,%C3%A0moyentermeauQu%C3%A9bec>.

66 C. Guay, M. Minville and M. Braun, A global portrait of hydrological changes at the 2050 horizon for the province of Québec, *Can. Water Resour. J.*, 2015, **40**(3), 285–302.

67 G. B. Lawrence and K. M. Roy, Ongoing increases in dissolved organic carbon are sustained by decreases in ionic strength rather than decreased acidity in waters recovering from acidic deposition, *Sci. Total Environ.*, 2021, **766**, 142529.

68 O. Pourret, M. Davranche, G. Gruau and A. Dia, Rare earth elements complexation with humic acid, *Chem. Geol.*, 2007, **243**(1–2), 128–141.

69 C. Catrouillet, H. Guenet, A.-C. Pierson-Wickmann, A. Dia, M. B. LeCoz, S. Deville, *et al.*, Rare earth elements as tracers of active colloidal organic matter composition, *Environ. Chem.*, 2020, **17**(2), 133–139.



70 C. Jiang, Y. Li, C. Li, L. Zheng and L. Zheng, Distribution, source and behavior of rare earth elements in surface water and sediments in a subtropical freshwater lake influenced by human activities, *Environ. Pollut.*, 2022, **313**, 120153.

71 M. Davranche, O. Pourret, G. Gruau and A. Dia, Impact of humate complexation on the adsorption of REE onto Fe oxyhydroxide, *J. Colloid Interface Sci.*, 2004, **277**(2), 271–279.

72 da S. YJAB, C. W. A. do Nascimento, Y. J. A. B. da Silva, F. F. Amorim, J. R. B. Cantalice, V. P. Singh, *et al.*, Bed and suspended sediment-associated rare earth element concentrations and fluxes in a polluted Brazilian river system, *Environ. Sci. Pollut. Res.*, 2018, **25**(34), 34426–34437.

73 K. H. Johannesson, D. A. Chevis, D. J. Burdige, J. E. Cable, J. B. Martin and M. Roy, Submarine groundwater discharge is an important net source of light and middle REEs to coastal waters of the Indian River Lagoon, Florida, USA, *Geochim. Cosmochim. Acta*, 2011, **75**(3), 825–843.

74 U. Lueder, B. B. Jørgensen, A. Kappler and C. Schmidt, Photochemistry of iron in aquatic environments, *Environ. Sci.: Processes Impacts*, 2020, **22**(1), 12–24.

75 Y. Lv, J. Liu, R. Zhu, J. Zhu, Q. Chen, X. Liang, *et al.*, Photoreductive Dissolution of Iron (Hydr)oxides and Its Geochemical Significance, *ACS Earth Space Chem.*, 2022, **6**(4), 811–829.

76 J. Viers, B. Dupré and J. Gaillardet, Chemical composition of suspended sediments in World Rivers: new insights from a new database, *Sci. Total Environ.*, 2009, **407**(2), 853–868.

77 B. Rondeau, D. Cossa, P. Gagnon and L. Bilodeau, Budget and sources of suspended sediment transported in the St. Lawrence River, Canada, *Hydrol. Processes*, 2000, **14**(1), 21–36.

78 A. Xu, E. Hathorne, G. Laukert and M. Frank, Overlooked riverine contributions of dissolved neodymium and hafnium to the Amazon estuary and oceans, *Nat. Commun.*, 2023, **14**(1), 4156.

79 N. L. Poff and D. D. Hart, How Dams Vary and Why It Matters for the Emerging Science of Dam Removal: an ecological classification of dams is needed to characterize how the tremendous variation in the size, operational mode, age, and number of dams in a river basin influences the potential for restoring regulated rivers via dam removal, *BioScience*, 2002, **52**(8), 659–668.

80 L. A. Martin, D. A. L. Vignati and C. Hissler, Contrasting distribution of REE and yttrium among particulate, colloidal and dissolved fractions during low and high flows in peri-urban and agricultural river systems, *Sci. Total Environ.*, 2021, **790**, 148207.

81 K. Inoue, M. Fukushi, A. Furukawa, S. K. Sahoo, N. Veerasamy, K. Ichimura, *et al.*, Impact on gadolinium anomaly in river waters in Tokyo related to the increased number of MRI devices in use, *Mar. Pollut. Bull.*, 2020, **154**, 111148.

